

# MACHINE LEARNING OF ELECTROENCEPHALOGRAPHY SIGNALS AND EYE MOVEMENTS TO CLASSIFY WORK-IN-PROGRESS RISK AT CONSTRUCTION SITES

Jui-Sheng CHOU<sup>1</sup> , Pin-Chao LIAO<sup>2</sup>, Chi-Yun LIU<sup>1</sup>, Chia-Yung HOU<sup>1</sup>

<sup>1</sup>Department of Civil and Construction Engineering, National Taiwan University of Science and Technology, Taipei, Taiwan

<sup>2</sup>Department of Construction Management, Tsinghua University, Beijing, China

## Article History:

- received 24 December 2023
- accepted 19 August 2024
- first published online 31 December 2024

**Abstract.** The construction industry has consistently faced high accident rates and delays in recognizing hazards, posing significant risks to onsite personnel. Traditional hazard detection methods are often reactive rather than proactive, emphasizing a pressing need for innovative solutions. Despite advances in safety technology, a considerable gap remains in real-time, accurate hazard recognition at construction sites. Current technologies do not fully leverage physiological data to predict and mitigate risks. This research introduces a groundbreaking approach by employing machine learning to analyze electroencephalography (EEG) signals and eye movement data, enabling real-time differentiation of safe, warning, and hazardous visual cues. A Random Forest model with an impressive classification accuracy of 99.04% has been developed, marking a significant enhancement in identifying potential hazards. The possible impact of integrating EEG and eye movement analyses into wearable devices or onsite sensors is substantial, as it could revolutionize safety protocols in the construction industry, fostering a safer future.

**Keywords:** construction safety, brain-computer interface, electroencephalography (EEG), eye movement, machine learning, construction site hazard recognition.

✉ Corresponding author. E-mail: [jschou@mail.ntust.edu.tw](mailto:jschou@mail.ntust.edu.tw)

## 1. Introduction

The construction industry has long been plagued by a significantly high number of work-related fatalities, as shown in Figure 1. Over the past nine years, Taiwan alone has reported 2,879 deaths, with nearly half occurring in this sector (Occupational Safety and Health Administration, 2020). Human error accounts for approximately 80% of these accidents, and there is a notable delay in recognizing hazards, with 57% of dangers not identified promptly (Garrett & Teizer, 2009). These statistics underscore the urgent and pressing need for enhanced safety measures and innovative technologies to mitigate risks.

The high accident rates in construction highlight the insufficiency of current safety protocols and the urgent need for more effective hazard recognition strategies. This paper addresses these deficiencies by exploring the potential of hybrid brain-computer interfaces (BCIs) that integrate electroencephalography (EEG) and eye-tracking technologies (Liu et al., 2024). These technologies offer real-time monitoring and feedback capabilities that sig-

nificantly improve construction site hazard detection and response times.

EEG monitors brain activity to assess cognitive states such as alertness or fatigue, which are critical for accident prevention (Huang et al., 2024). Concurrently, eye-tracking technology monitors gaze direction to ensure workers remain focused on potential hazards (Larsen et al., 2024). Although these technologies have shown promise individually, their combined application in real-world construction settings remains limited. Recent studies suggest integrating EEG and eye-tracking systems can significantly enhance hazard detection and safety responses in high-risk environments (Cheng et al., 2022; Vortmann et al., 2022). However, the widespread adoption of these systems in construction is lacking, and their full potential has yet to be realized.

This research addresses these gaps by advancing the development of wearable BCIs specifically designed for construction sites. Our approach synergizes EEG and eye-

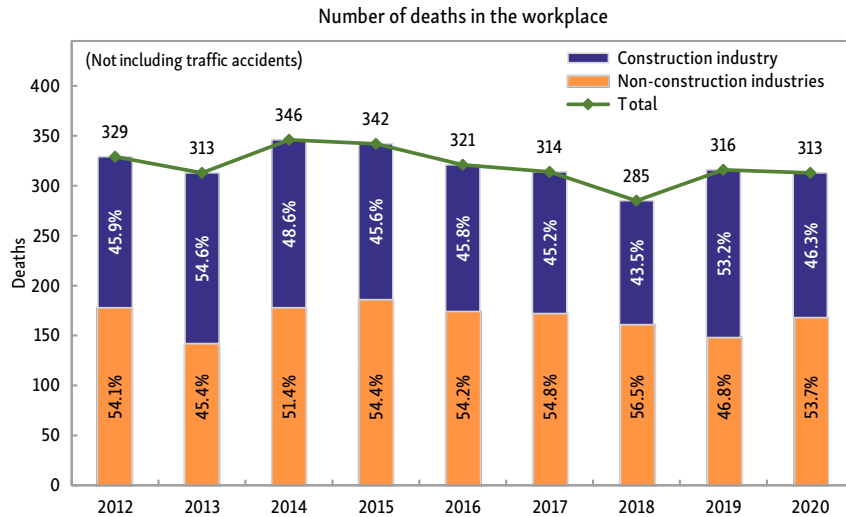


Figure 1. Statistics on work-related deaths from Annual Labor Inspection Report

tracking data to improve situational awareness and hazard detection. We utilize machine learning (ML) models to analyze EEG signals and eye movements, enabling construction workers to detect real-time safety, warning, or hazard signals. By building on Hans Berger’s foundational work in EEG technology and leveraging modern advancements in machine learning and eye-tracking accuracy (Ince et al., 2021), this study proposes a novel solution to enhance construction site safety.

Reflecting on the foundational work by Hans Berger in EEG technology, which has been applied in various fields since 1929, from clinical research to marketing (Behzadnia et al., 2017; Vecchiato et al., 2011), our study builds on a rich history of technological innovation. The detailed

structure of the brain, with its two hemispheres and four lobes – frontal, parietal, occipital, and temporal – is integral to understanding how these tools can be applied effectively in hazard recognition (Bui & Das, 2022), as shown in Figure 2. Modern EEG caps, designed using the International 10–20 system, ensure precise electrode placement for comprehensive data collection (Klem et al., 1961), as illustrated in Figure 3.

From 2017 to 2021, significant technological strides have been made, from Saghafi et al. (2017) real-time eye status detection with 88.2% accuracy to Noghabaei et al. (2021) application of machine learning to predict hazards with up to 98.6% accuracy in immersive environments. These advancements underscore the transformative potential of integrating machine learning with EEG and eye-tracking to enhance construction safety, promising a safer future for the industry.

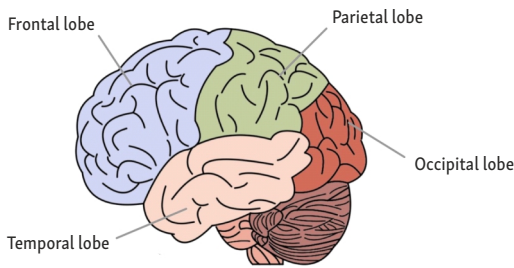


Figure 2. Structure of cerebrum

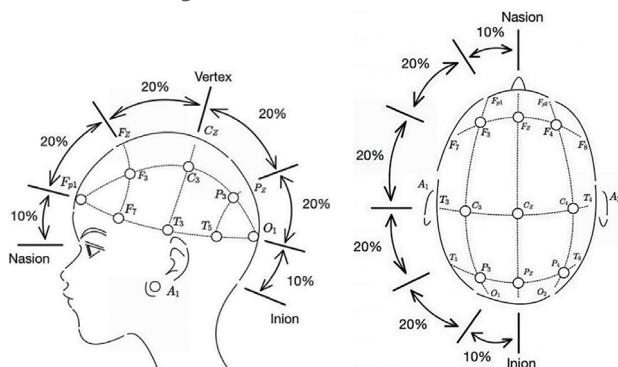


Figure 3. International 10–20 electrode system

## 2. Research method and data collection

### 2.1. Analysis tool

The analysis tool adopted in this study was the Waikato Environment for Knowledge Analysis (WEKA) (Hall et al., 2009). WEKA was used to construct and compare models for onsite hazard recognition in the presence of potential construction site hazards. The details of the ML model parameters are provided in Appendix, Table A1. The model that best fits is recommended.

### 2.2. Machine learning

The study utilizes several established machine learning models to analyze data, each chosen for its specific advantages in addressing various aspects of construction site data, thereby enhancing our analytical precision and depth:

- **Decision Trees (J48):** This model classifies data by generating a tree structure based on training data rules (Moore II, 1987).

- **Bayesian Networks (BayesNet):** Leveraging probability theory, this model assesses risks and makes predictions based on known conditions (Rosen & Krithivasan, 2012).
- **Artificial Neural Networks (ANNs):** Inspired by biological neural networks, ANNs process inputs through multiple layers to produce outputs (McCulloch & Pitts, 1943).
- **REPTree:** Renowned for its efficient tree construction and reduced-error pruning, this is a variant of the traditional decision tree (Mohamed et al., 2012).
- **Logistic Regression:** Adapting linear regression, this model classifies data into discrete categories (Hosmer Jr et al., 2013).
- **Support Vector Machines (SVM):** SVMs classify data by mapping it into a higher-dimensional space to create a separating hyperplane (Smola & Vapnik, 1997).
- **Random Forest:** An ensemble of decision trees, this model is designed to increase predictive accuracy and robustness (Liu et al., 2021).

### 2.3. Model validation and error evaluation criteria

After establishing the models, their performance and accuracy were compared. The reliability of the models was validated, and their errors were evaluated using cross-validation and performance-evaluation indices.

#### 2.3.1. Cross-validation

K-fold cross-validation was applied to test individual models or compare the stability of two or more prediction models. It is particularly suitable for small datasets and makes good use of the information contained in each data item (Wei, 2021). This approach randomly divides the data into K subsets that alternately serve as training and test sets. Ten-fold cross-validation was employed, where the same model was trained using ten subsets. During each

round of training, nine of the ten subsets served as the training set; the remaining subset did not participate in training and served as the validation test set. Thus, in ten training rounds, there are ten errors from ten different validation sets. The performance of the model is the mean of these errors. The model's average accuracy and robustness (reliability) can be assessed using the mean and standard deviation of the loss function values from the ten rounds.

#### 2.3.2. Classification evaluation indices

In all classification problems, a confusion matrix is generated. From this matrix, performance indices such as True Positive (TP), True Negative (TN), False Positive (FP), and False Negative (FN) can be calculated. Imbalanced classes were not observed because the datasets exhibited a somewhat normal distribution. Consequently, only the primary classification evaluation metric, namely accuracy  $\left( \frac{TP + TN}{TP + TN + FP + FN} \right)$ , was employed to evaluate the prediction error rates of the classification models (Gong et al., 2020).

### 2.4. Data collection and preprocessing

The primary objective of this study was to determine the relationship between on-site hazard recognition and the characteristics of brain activity and eye movements. During data collection, brain signals, eye movements, and hand button responses formed synchronous data, compensating for the inadequacies of single physiological responses, thereby enabling the assessment of participants' safety awareness when viewing different hazardous workplaces. The participants were briefed on the experimental procedure (Figure 4), which encompassed background information about the participants, the experimental instruments and models, and the 120 pictures they viewed. Examples of construction site hazard photographs are provided in Figure A.1, illustrating hazardous conditions, and Figure A.2, depicting safe conditions in the Appendix.

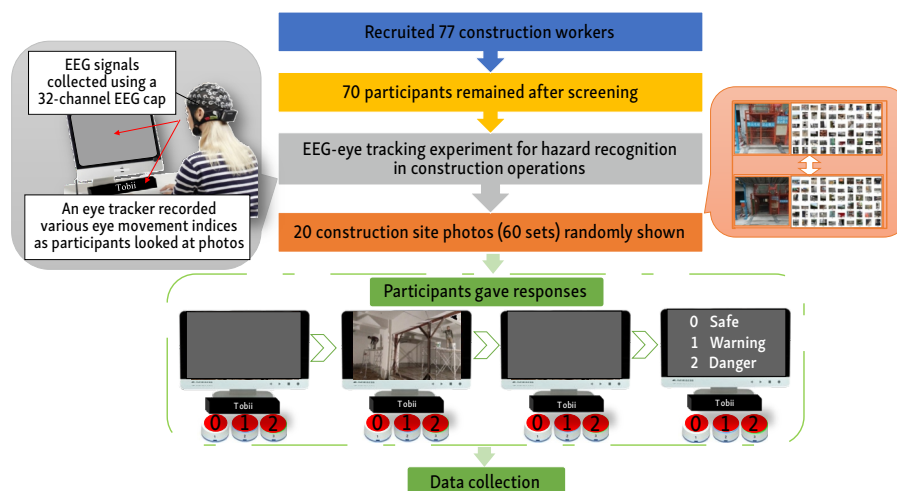


Figure 4. Experimental procedure combining EEG signals and eye movement for hazard recognition in construction operations

## 2.4.1. EEG-eye tracking experiment

### 2.4.1.1. Details related to participant background and experiment instruments

The data analysis for this study was carried out on a participant randomly selected from a pool of 70. This participant, a 52-year-old construction worker with 22 years of experience, evaluated 120 images and achieved an accuracy rate of 69.17% (83 correct responses and 37 incorrect responses). An in-depth examination of this case provides valuable insights into specific cognitive patterns and reactions within hazard recognition scenarios.

Future research could involve a larger pool of participants to validate further and enhance these preliminary findings. This expanded approach would allow for a more thorough assessment of the hazard recognition model's applicability across various demographics within the construction industry, thereby improving its practicality and effectiveness in enhancing safety measures.

Figure 5 shows the instruments and models employed in the experiment. The device at the top is an EEG cap (Neuracle NeuSen W), and the one below is an eye tracker (Tobii X320). Figure 6 shows the distributions of the EEG channels of the EEG cap used in this study. Based on the

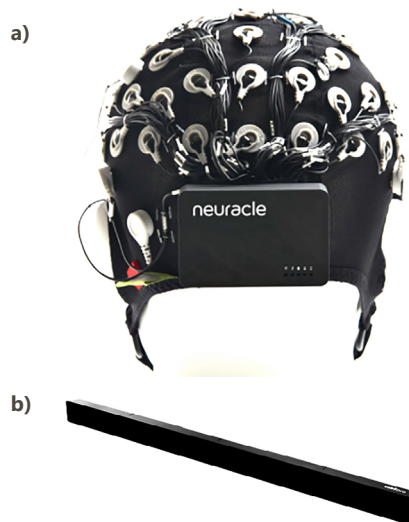


**Figure 5.** Experiment instruments: a – EEG cap (Neuracle NeuSen W); b – Eye tracker (Tobii X320)

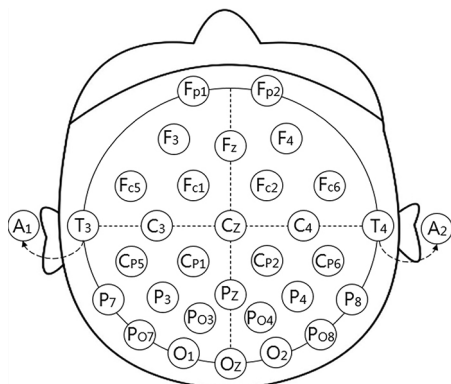


**Figure 6.** Diagram of EEG channels

International 10–20 system, the electrodes are positioned at Fp1, Fp2, F3, F4, Fz, Fc1, Fc2, Fc5, Fc6, T3, T4, C3, C4, Cz, Cp1, Cp2, Cp5, Cp6, P3, P4, Pz, P7, P8, Po3, Po4, Po7, Po8, O1, O2, Oz, A1, and A2, comprising 32 EEG channels.

### 2.4.1.2. Experiment images

Each participant was shown 60 sets of construction site photographs. As shown in Table 1, each set contains images of both hazardous and safe conditions. The hazards within these 60 sets were categorized into five groups: (1) electric shock, (2) falls, (3) collapsing frames, (4) falling objects, and (5) others. Table 1 details the risks identified in construction work environments, explaining the primary sources of construction hazards and the prevention principles. Table 2 presents the descriptive statistics of the image dataset according to hazard type.

**Table 1.** Construction operating risk recognition






Main impact	Source of hazard
Electric shock	Electromechanical equipment, overhead high-voltage lines, underground high-voltage lines, power supply equipment, damaged wires on the ground, and wet indoor operation ground
Falls	Openings in floors, openings for elevators and pipelines, operations on temporary work platforms, lack of safety protection sheds at ground entrances/exits of construction elevators
Collapsing frames	Floor support frames, floorboards, construction frames
Falling objects	Lack of safety regulation compliance with safety ropes and hooks in lifting operations, mobile cranes, and lifting materials
Others	Unorganized material placing, unremoved debris, insufficient warning signs, exposed rebar in slope support, workers not wearing safety helmets

### 2.4.1.3. Experimental procedure

Initially, 77 male construction workers were recruited. After the screening, we excluded one participant whose EEG signals contained too many artifacts, which affected over 50% of the results. Next, we released a project manager who was not an onsite worker. Finally, we dropped five participants whose validation test data needed to be more reliable. The final sample size of our experiment was 70 participants, whose ages ranged from 21 to 60, with a mean of 42.

During the EEG eye-tracking experiment, participants were presented with 60 sets (120 images) of 2D photographs depicting construction sites displayed in random order. They were required to determine the presence of hazards based solely on their prior experience. This design choice mirrors real-world conditions where construction workers rely on their instincts and expertise for hazard recognition. This approach ensures that the data collected reflects genuine, spontaneous responses to potential hazards, which is crucial for developing an effective hazard recognition model suitable for realistic settings. Par-

**Table 2.** Descriptive statistics of hazard types

Hazard type	Electric shock	Falls	Collapsing frames	Falling objects	Others
Number of images	28	36	12	20	24
Example photo					
Description	Lack of gate or rainproof measures on the distribution box	Lack of protection measures over the basement sump hole	Lack of tie rod on elevator opening frame	Fixed location of a bucket lift safety rope not compliant with safety regulations	Construction workers are not wearing safety helmets or protective gear.

Participants expressed their evaluations by pressing a button, classifying the conditions depicted in the images as safe, worthy of caution, or hazardous.

This setup, which purposefully refrained from informing or training participants about the labels of hazards before the experiment, was designed to elicit intuitive and unaided responses. This method is instrumental in assessing workers' natural proficiency and limitations in hazard recognition, providing valuable insights for developing targeted training programs to address specific weaknesses.

The 120 photographs of the construction sites were shown to the participants in random order. Each test began with a blank white screen for 0.5 seconds, followed by a construction site image for a maximum of 3 seconds, another blank white screen for 0.5 seconds, and then the final response screen. The participants responded by instructions (0 indicating safe, 1 indicating worthy of caution, and 2 indicating hazardous), as shown in Figure 7. Each participant took approximately 40 minutes to complete the experiment.

#### 2.4.2. Data preprocessing

During the hazard recognition experiment, EEG signals were collected from participants using an EEG cap while their eye activities were concurrently monitored with an eye tracker. The training dataset comprised 36 variables, including signals from 32 EEG channels and four indices of eye movement: type of eye activity, Area of Interest (AOI), and the diameters of the left and right pupils. The EEG cap operated at a sampling frequency of 250 Hz, capturing

data every four milliseconds and accumulating 233,500 original data points. In contrast, the eye tracker functioned at a frequency of 120 Hz, recording data every eight milliseconds, yielding 103,980 original data points.

To synchronize the EEG and eye movement datasets, we merged them using the least common multiple of their sampling intervals, eight milliseconds. Missing values, inevitable during signal transmission, were identified and systematically removed. This refinement process resulted in a final dataset comprising 35,700 data points for our classification model.

In the preprocessing stage, the EEG signals underwent band-pass filtering to retain only frequencies between 1 Hz and 40 Hz, which is crucial for cognitive processing. This filtering was pivotal in minimizing high-frequency noise and slow-drift artifacts. Independent Component Analysis (ICA) was subsequently applied to isolate and eliminate artifacts associated with eye movements, muscle activities, and external electrical noises, ensuring the integrity of the brain activity signals for reliable analysis.

Moreover, the EEG data were segmented into epochs centered around the stimulus onset, each spanning from 200 milliseconds before to 800 milliseconds after the stimulus. Each epoch was baseline-corrected using the pre-stimulus period to adjust for signal variations and drifts, which is crucial for ensuring consistency across trials. These preprocessing steps, validated by recent research, have significantly enhanced the quality of the EEG data for constructing robust hazard classification models (Liao et al., 2022).

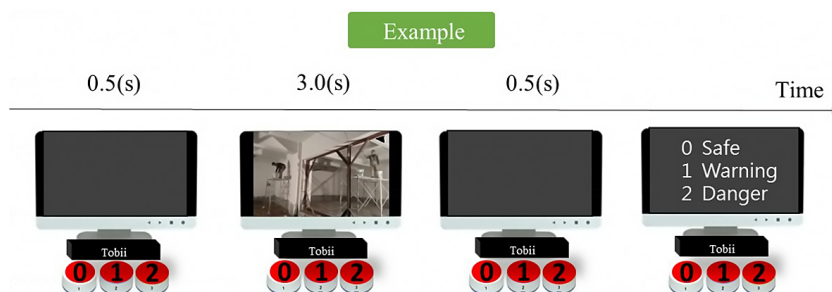
**Figure 7.** Example of participant giving responses during the experiment

Table 3. Factors adopted for the classification model

Function		EEG factors	Channel function	Unit	Variable symbol	Description	Minimum value	Maximum value	Mean	SD (Standard deviation)
Stress detection		FC1	Motor control	Microvolt (µV)	X6	Names of EEG channels: F: frontal lobe; P: parietal lobe; O: occipital lobe; T: temporal lobe; C: central; Z: zero.	9,469	10,561	9,972	273
		FC2	Motor control		X7		-1,846	-455	-1,038	416
		FC5	Problem-solving		X8		615	3,024	1,731	630
		FC6	Problem-solving		X9		1,496	2,032	1,895	59
		C3	Sensory motion (right)		X11		-5,923	-5,369	-5,684	82
		C4	Sensory motion (left)		X12		-537	153	-101	149
		T3	Lingual and visual memory		X13		-1,735	153	-560	506
		T4	Emotional memory		X14		4,151	5,281	4,839	119
		CP1	Proprioception		X15		-375,000	374,999	35,236	49,608
		CP2	Proprioception		X16		-375,000	374,999	30,206	51,087
		CP5	Spatial perception		X17		-3,687	-2,708	-3,087	215
		CP6	Spatial perception		X18		-2,468	294	-931	956
		P3	Lingual logic and cognition		X20		4,740	5,265	5,027	132
		P4	Mathematical logic and cognition		X21		8,092	8,446	8,321	67
		P7	Spatial and visual processing		X22		7,169	8,170	7,582	255
		P8	Spatial and visual processing		X23		-8,239	-4,095	-5,893	1,157
Stress detection	Emotional state	F3	Motion planning	X4	5,621	6,229	5,955	148		
		F4	Motion planning	X5	-358	590	-119	147		
Reading ability		PO3	Visual memory	X24	639	1,723	1,209	202		
		PO4	Visual memory	X25	-5,782	-4,991	-5,281	152		
		PO7	Language comprehension	X26	864	3,924	2,040	713		
		PO8	Language comprehension	X27	-15,634	-15,047	-15,276	122		
Hazard recognition		O1	Visual information processing	Microvolt (µV)	X29	Names of EEG channels: F: frontal lobe; P: parietal lobe; O: occipital lobe; T: temporal lobe; C: central; Z: zero.	-4,991	-3,017	-3,999	494
		O2	Visual information processing		X30		-13,294	-10,775	-11,991	642
		Oz	Visual information processing		X28		4,881	6,379	5,855	405
Emotional state		Fz	Working memory	X3	8,578	9,115	8,860	155		
Reference electrodes		A1	Ear reference electrode	X31	-5,131	-2,598	-4,024	681		
		A2	Ear reference electrode	X32	-3,071	-922	-1,807	628		
Sensory cognition		Cz	Sensory motion	X10	4,206	4,829	4,560	157		
		Pz	Cognitive processing	X19	4,440	4,973	4,730	104		
Fatigue detection		Fp1	Attention	X1	-10,081	-4,991	-8,924	626		
		Fp2	Judgment	X2	-15,908	-14,746	-15,134	654		
Eye movement characteristics	Fixation; saccades; unclassified	-	-	X33	Eye movements are divided into fixation, saccades, and unclassified	-				
	AOI	-	-	X34	0 and 1 indicate whether the fixation point falls within a designated area in the photos: 1 if it does, and 0 otherwise	-				
	Left and right pupil diameters	-	mm	X35; X36	Two factors: diameters of left and right pupils	1.51	5.51	2.97	0.414	
						1.35	4.80	2.96	0.339	
Hazard recognition	Safe; worthy of caution; hazardous	-	-	Y	The participant's response may be safe, worthy of caution, or hazardous.	-				

Table 3 offers a detailed analysis of the variables used in the classification model, including the 32 EEG channels, types of eye movements (saccades, fixation, and unclassified), AOI, and pupil diameters. These variables were effectively employed to predict hazard recognition capabilities among construction workers.

### 3. Developing onsite hazard classification models using EEG and eye-tracking data

Section 3 details the development of onsite hazard classification models utilizing EEG signals facilitated by the WEKA platform. This initiative is critical for enhancing hazard recognition among construction workers. The models, extensively detailed in Table 4, illustrate the selection of factors used for algorithm analysis and explain the objectives of each model. By integrating both EEG and eye-tracking data, these models leverage the complementary strengths of these technologies to improve the robustness and accuracy of hazard detection. This integration within the WEKA platform has led to the creation of advanced algorithms tailored explicitly for construction sites' dynamic and complex environments, ensuring that safety protocols are proactive and reactive.

Combining EEG and eye-tracking data enriches our understanding of workers' attentional focus and cognitive engagement with potential hazards. While EEG data alone may not reliably pinpoint a worker's attentional focus or identify specific environmental triggers, eye-tracking provides insights into where attention is directed but may lack depth in revealing cognitive and emotional responses. Together, these methods offer a comprehensive perspective that significantly enhances hazard detection capabilities.

Our comparative studies, outlined in 'Section 3.4' of Table 4, explore the synergistic benefits of integrating EEG and eye-tracking data compared to using a single data source. This analysis aims to determine how this integrated

approach improves the reliability of hazard recognition, a vital component in advancing safety measures on construction sites.

Additionally, employing EEG and eye-tracking data facilitates the development of sophisticated, adaptive safety systems that deliver real-time feedback and alerts to construction workers. This approach not only aids in immediate hazard detection but also promotes long-term behavioral adjustments, significantly reducing the incidence of accidents on construction sites.

#### 3.1. Comparison of single and ensemble models

Classification predictions were initially conducted using all EEG channels with seven of the most commonly employed algorithms from WEKA literature. These models include J48, BayesNet, ANN, REPTree, LR, SVM, and Random Forest. Cross-validation was used to compare their prediction accuracy and assess model stability. The results indicate that the Random Forest model achieved an average accuracy of 99.9% with a standard deviation of 0.057% in hazard recognition, using 32 channels of EEG signals. According to Table 5, Random Forest was the best classification model.

#### 3.2. Optimization of EEG channels for hazard recognition

Each EEG channel corresponds to a distinct physiological response, covering a broad spectrum of EEG channels. Understanding the influence of various sensory channel factors on hazard recognition would help to identify optimal EEG channel combinations. The 32 channels recorded with the EEG cap in this study were categorized into the following functional areas: stress detection, emotional state, hazard recognition, fatigue detection, sensory cognition, reading ability, and reference electrodes (Noghabaei et al., 2021; Saedi et al., 2022).

**Table 4.** Summary table of classification models

Section	Activity summary	Validation method	Algorithms	Purpose
3.1	All EEG channels are initially used for hazard recognition, and the accuracy and stability of seven classifiers are compared.	Ten-fold cross-validation	J48, BayesNet, ANN, REPTree, LR, SVM, Random Forest	To perform a preliminary analysis to select the best classifier (the tested classifiers are all more common techniques in reviewed literature).
3.2	Hazard classification (safe, worthy of caution, and hazardous) is performed by differentiating physiological responses corresponding to 10 EEG channels.			To test the influence of factors on model classification accuracy based on EEG channel function.
3.3	Sensitivity analysis is performed using EEG factors suggested in the literature to examine the impact of individual characteristics on model classification accuracy.			Adopting a parsimonious number of EEG channels to achieve adequate prediction accuracy with reasonable modeling costs is necessary.
3.4	Hazard recognition is performed using EEG channels and eye movement characteristics.			Evaluating the enhancement of classification accuracy by integrating EEG and eye movement data in on-site hazard recognition.

**Table 5.** Analysis of seven WEKA classifiers trained using ten-fold cross-validation and 32 EEG channels

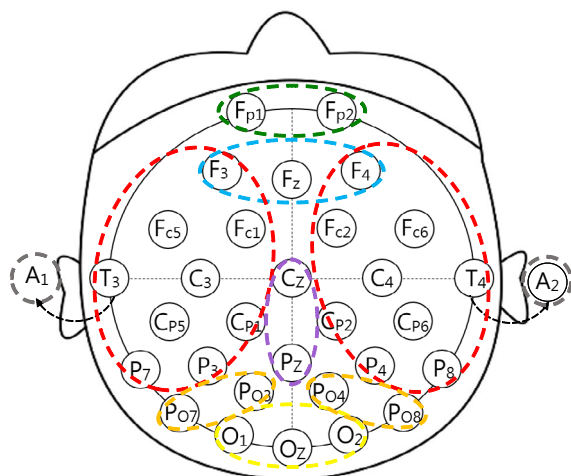
Classifier	Modeling time (sec)	Average classification accuracy rate (%)	SD (%)
J48	3.67	98.9	0.264
BayesNet	0.61	89.71	10.470
ANN	142.69	99.2	0.231
REPTree	0.99	98.5	0.351
LR	4.43	64.3	5.139
SVM	153.87	61.9	35.161
Random Forest	16.38	99.9	0.057

Figure 8 shows the locations of the EEG electrodes grouped according to their functional areas, with the corresponding colors listed in Table 6. Next, based on EEG channel functions and suggestions in the literature (Noghabaei et al., 2021; Saedi et al., 2022), we investigated the influence of different factor combinations on the classification accuracy of the hazard recognition model.

The ML model training results, considering all or a screened portion of the factors, are presented in Table 7. The baseline model was initially examined, where all channel features were used as input factors. Parsimonious feature-channel combinations were tested for accuracy to minimize data collection expenses.

The preliminary analysis showed that the baseline model achieved a hazard recognition classification accuracy of 99.98%, with Random Forest identified as the optimal training model. The second-best model, which utilized stress-detection feature channels (18 EEG channels), achieved a classification accuracy of 99.96% in hazard recognition. Using only four reading-ability feature channels, the third-best model achieved a classification accuracy of

Stress detection (P)	Reading ability (R)	Hazard recognition (D)	Emotional state (E)	Reference electrodes (Re)	Sensory cognition (Pe)	Fatigue detection (F)



**Figure 8.** EEG electrode locations grouped by functional area

97.92%. The analysis of the hazard-recognition feature indicated that the three EEG channels could provide a classification accuracy of 90.28%.

Next, the factors and hazard awareness-related EEG channels proposed by Saedi et al. (2022) and Noghabaei et al. (2021) were incorporated. The results revealed that using the ten EEG channels suggested by Saedi et al. (2022) (FC5, FC6, P7, P8, F3, F4, O1, O2, Fp1, and Fp2) achieved a classification accuracy of 99.49%. However, adopting the three EEG channels suggested by Noghabaei et al. (2021) (FC5, O1, and O2) achieved a classification accuracy of 90.94%.

**Table 6.** EEG features corresponding to channel functions

EEG feature	Channel function	Color corresponding to the sensory channel
FC1	Motor control	
FC2	Motor control	
FC5	Problem-solving	
FC6	Problem-solving	
C3	Sensory motion (right)	
C4	Sensory motion (left)	
T3	Lingual and visual memory	
T4	Emotional memory	
CP1	Proprioception	
CP2	Proprioception	
CP5	Spatial perception	
CP6	Spatial perception	
P3	Lingual logic and cognition	
P4	Mathematical logic and cognition	
P7	Spatial and visual processing	
P8	Spatial and visual processing	
F3	Motion planning	
F4	Motion planning	
PO3	Visual memory	
PO4	Visual memory	
PO7	Language comprehension	
PO8	Language comprehension	
O1	Visual information processing	
O2	Visual information processing	
Oz	Visual information processing	
Fz	Working memory	
A1	Ear reference electrode	
A2	Ear reference electrode	
Cz	Sensory motion	
Pz	Cognitive processing	
Fp1	Attention	
Fp2	Judgment	



**Table 7.** ML model training results based on considering all or a portion of the factors screened according to channel function

	Channel function	All channels	Stress detection	Reading ability	Hazard recognition	Emotional state	Reference electrodes	Sensory cognition	Fatigue detection	Saedi et al. (2022)	Nogha-baei et al. (2021)
FC1	Motor control	V	V								
FC2	Motor control	V	V								
FC5	Problem-solving	V	V							V	V
FC6	Problem-solving	V	V							V	
C3	Sensory motion (right)	V	V								
C4	Sensory motion (left)	V	V								
T3	Lingual and visual memory	V	V								
T4	Emotional memory	V	V								
CP1	Proprioception	V	V								
CP2	Proprioception	V	V								
CP5	Spatial perception	V	V								
CP6	Spatial perception	V	V								
P3	Lingual logic and cognition	V	V								
P4	Mathematical logic and cognition	V	V								
P7	Spatial and visual processing	V	V							V	
P8	Spatial and visual processing	V	V							V	
F3	Motion planning	V	V			V				V	
F4	Motion planning	V	V			V				V	
PO3	Visual memory	V		V							
PO4	Visual memory	V		V							
PO7	Language comprehension	V		V							
PO8	Language comprehension	V		V							
O1	Visual information processing	V			V					V	V
O2	Visual information processing	V			V					V	V
Oz	Visual information processing	V			V						
Fz	Working memory	V				V					
A1	Ear reference electrode	V					V				
A2	Ear reference electrode	V					V				
Cz	Sensory motion	V						V			
Pz	Cognitive processing	V						V			
Fp1	Attention	V							V	V	
Fp2	Judgment	V							V	V	
Total number of factors (channels)		32	18	4	3	3	2	2	2	10	3
Optimal algorithm		Random Forest	Random Forest	Random Forest	Random Forest	Random Forest	J48	J48	J48	Random Forest	Random Forest
Average accuracy rate (%)		99.98	99.96	97.92	90.28	78.99	86.92	78.38	71.59	99.49	90.94
SD (%)		0.057	0.056	0.656	3.664	7.267	4.020	7.803	8.398	0.116	3.828
Model training time (sec)		16.38	11.81	8.88	6.52	6.91	0.58	0.67	0.45	10.94	6.34

### 3.3. Sensitivity of model accuracy to EEG channels

Accuracy was employed as the evaluation criterion to assess the influence of the EEG channel factor on the classification model predictions. With  $M$ , the performance value of the baseline model, as the benchmark, and  $M^*$ , the model's accuracy following the removal of factor  $i$ , we determined that the sensitivity of model accuracy to factor  $i$  is  $(M^* - M)/M$ . By definition, a factor positively influences model accuracy when its removal causes the model's prediction accuracy to decrease; thus, its presence increases the accuracy of model classification. If the accuracy reduces significantly, the factor positively influences the prediction model.

The analysis revealed that using the ten EEG features suggested by Saedi et al. (2022) achieved an accuracy of 99.49%. We adopted this model as our baseline and evaluated the impact of different factors on model prediction for statistical parsimony analysis to achieve adequate accuracy with the minimum amount of data. We employed ten-fold cross-validation to test the feature sensitivity, as shown in Figure 9. The vertical axis represents the average accuracy, and the horizontal axis represents the removed factor. "BL" represents the baseline model, with no factors eliminated. The graph demonstrates that all factors exerted varying degrees of positive influence on the model's classification accuracy. If the collection of EEG channel features is subject to limitations or data acquisition cost considerations,

critical factors selected based on their degree of influence can be collected first, and the adequacy of the resulting model prediction accuracy can be assessed afterward.

Figure 10 shows the accuracy of classification models constructed using ten-fold cross-validation and the positive influence factors ranked by the suggested feature channel data. The results show that using the top-six positive influencing factors achieved an accuracy of 99.04%. These factors included the EEG channels with stress detection (P8, P7, and FC5), hazard recognition (O2 and O1), and fatigue detection (Fp1) functions. We can balance model quality and electrode count by selecting these six channels, offering an optimal trade-off between cost and accuracy. This investigation also indicates that accuracy decreases significantly when the number of EEG factors is less than three, based on the ten EEG features recommended by Saedi et al. (2022).

Figure 11 provides a comprehensive view of the accuracy trends in our hazard recognition models, which are influenced by the number of EEG channels used across various brain regions. For instance, when four factors are used, the "Reading Ability" (R) functional area demonstrates a mean accuracy of 97.92%. With three factors, the channels recommended by Noghabaei et al. (2021) outperform others, achieving a mean accuracy of 90.94%. This finding highlights the role of different brain regions in the model's performance. Finally, when two factors are used, the mean accuracy for the "Reference Electrodes" (Re) functional area is 86.92%.

Rank	Positive influence factor
1	P8
2	P7
3	O2
4	FC5
5	Fp1
6	O1
7	F4
8	Fp2
9	FC6
10	F3

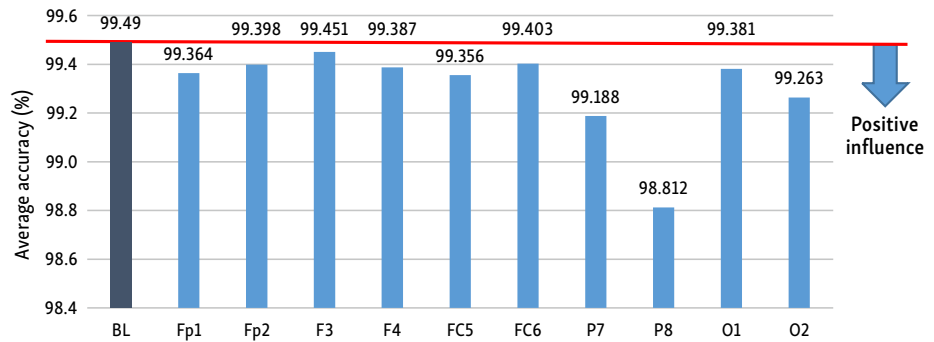


Figure 9. Sensitivity analysis of model prediction accuracy to removal of EEG channels

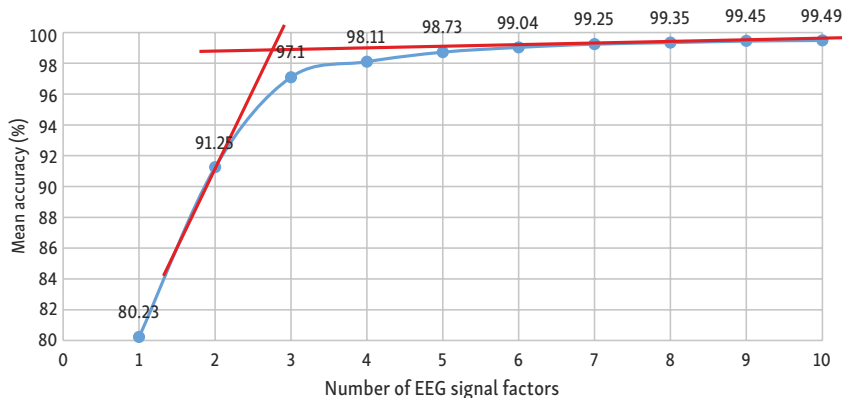


Figure 10. Average accuracy rates of classification models trained with varying numbers of positively influencing EEG channel factors

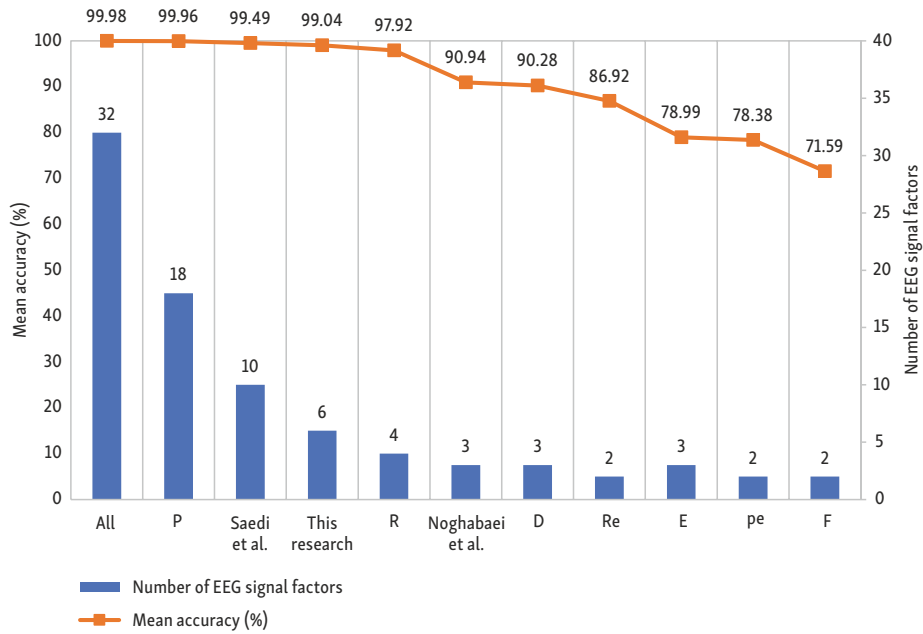


Figure 11. Classification model accuracy trends corresponding to different brain regions

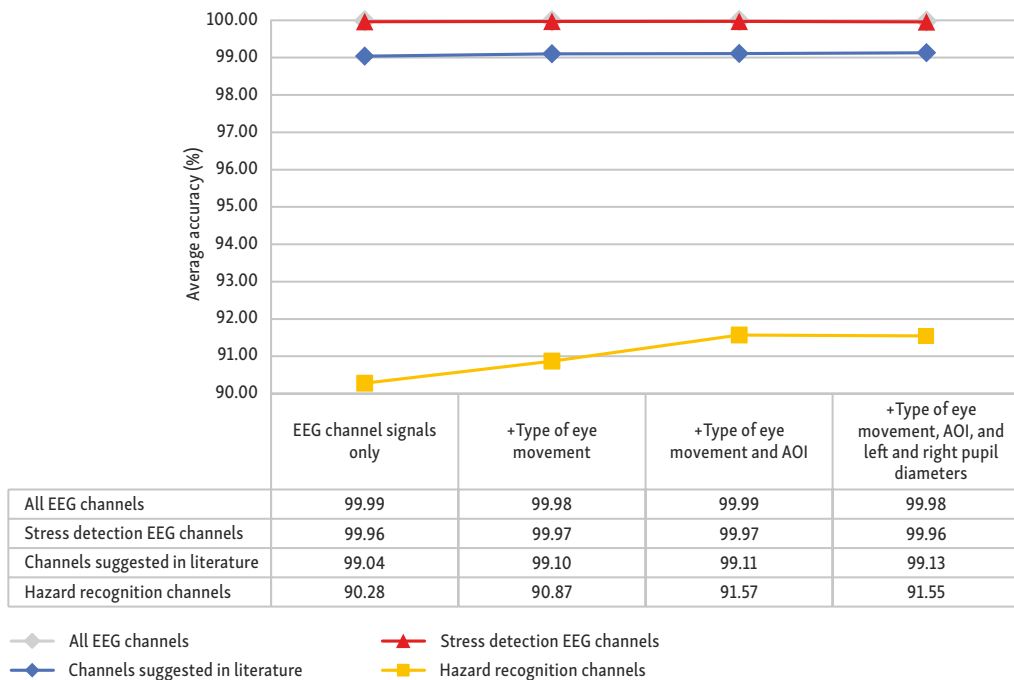


Figure 12. Comparison of model classification accuracy from combining EEG channel signals with eye movement characteristics

### 3.4. Modest gains in accuracy from integrating EEG and eye movement data

Our data analysis demonstrates that EEG channel features alone can provide satisfactory model performance. However, this section further explores the integration of specific EEG channel datasets with eye movement factor datasets to assess model classification accuracy thoroughly. The EEG channel datasets employed included all channels designated for stress detection, those recommended in the literature, and those targeted for hazard recognition.

We enhanced these datasets with eye movement characteristics, precisely the type of eye movement (fixation and saccades), area of interest (AOI), and pupil diameter, as depicted in Figure 12.

Including eye-tracking factors resulted in only a modest increase in accuracy. This observation highlights the potential benefits of incorporating eye-tracking data to enhance model performance. Specifically, when exclusively focusing on EEG channels associated with hazard recognition (O1, O2, and Oz) and combining them with eye movement factors for hazard identification, the classification ac-

curacy improved from 90.28% to 91.57%. Simultaneously, the error rate decreased by 13.3%. This empirical analysis suggests that while the combination of EEG signals with eye-tracking data does improve model accuracy, the enhancement in the accuracy of hazard recognition classification models is relatively minor.

#### 4. Conclusions and suggestions

This study underscores the efficacy of ensemble ML models in elucidating the complex interactions among various factors involved in onsite hazard recognition. Through the analysis of EEG signals and eye movement data, the research establishes a strong correlation between these factors and the accuracy of hazard recognition. Notably, specific EEG channels – P7, P8, FC5, O1, O2, and Fp1 – markedly improve classification accuracy, reaching an impressive 99.04%, with Random Forest models showing particular effectiveness.

Integrating EEG and eye-tracking data leverages the distinct benefits of each technology. EEG data provide insights into workers' cognitive and emotional states, while eye-tracking data pinpoint their focal points of attention. These datasets offer a comprehensive perspective that significantly bolsters hazard detection capabilities.

Further comparative studies reinforce the robustness of the Random Forest model. Utilizing 32 EEG channels, this model achieves an average accuracy of 99.9% with a very low standard deviation of 0.057%, highlighting the advantages of using extensive EEG data for precise hazard recognition.

The optimization of EEG channel selection is critical for practical applications. The research demonstrates that even a reduced subset of EEG channels – tailored to specific functions such as stress detection, hazard recognition, and fatigue monitoring – can maintain high accuracy while reducing data collection costs. For instance, using 18 channels for stress detection (P) reached 99.96% accuracy; 4 channels for assessing reading abilities (R) achieved 97.92% accuracy; and three channels for hazard recognition (D) attained 90.28% accuracy.

Sensitivity analysis further highlights the significant impact of specific EEG channels on model accuracy. For example, employing ten channels recommended by Saedi et al. (2022) resulted in a classification accuracy of 99.49%, while using three channels recommended by Noghabaei et al. (2021) achieved 90.94%. These findings suggest adopting a more focused and efficient data collection approach that emphasizes the most impactful channels to enhance model performance.

The study recommends prioritizing the integration of selected EEG and eye movement features to refine hazard recognition models specifically for construction applications. Streamlining data collection to focus on these key EEG channels could significantly reduce costs and complexity, making this advanced technology more practical for everyday use. The potential integration of biomechanical data with EEG and eye-tracking information could fur-

ther enhance these models, providing a more comprehensive understanding of worker states and improving hazard detection.

Advances in real-time data processing algorithms are essential as they could transform these models from static to dynamic, offering immediate feedback and revolutionizing safety protocols across various construction scenarios. The research also underscores a significant correlation between subjective responses and physiological measures, including EEG, eye movement, and pupil diameter, which are sensitive to brain responses before potential hazards are detected.

Future studies should explore the complex interactions among EEG channels, eye movements, and pupil diameter regarding construction site hazards, assessing their combined impact on visual responses. By aggregating data from a more significant number of subjects, researchers can minimize individual variances and derive more generalized, objective conclusions.

Further research might examine how different levels of work experience influence EEG and eye movement responses during hazard recognition tasks. Including participants with varying experience levels will provide deeper insights into the role of expertise in hazard recognition and enhance the practicality and effectiveness of safety measures.

The application of AI, mainly through developing sophisticated ML algorithms and integrating with the Internet of Things (IoT), holds significant promise for creating networked safety models that can anticipate and respond to hazards in real time. This advancement represents an important step forward in the development of intelligent construction sites.

Customizing hazard recognition models to suit specific construction environments and conducting longitudinal studies to assess the durability and effectiveness of wearable technologies under various conditions could address the unique challenges encountered in these settings, enhancing both safety and operational efficiency.

This study highlights the practical configurations that could transform construction management through enhanced human-computer interactions and advocates for broader adoption and further development of wearable EEG and eye-tracking technologies. These technologies significantly benefit the construction industry by improving worker safety and operational efficiencies.

#### Acknowledgements

The authors thank the National Science and Technology Council (110-2221-E-011-080-MY3), Taiwan, and the National Natural Science Foundation of China (No. 51878382) for financially supporting this research.

#### Competing interests

The authors declare that they have no known competing financial interests or personal relationships that could have appeared to influence the work reported in this paper.

## References

- Behzadnia, A., Ghoshuni, M., & Chermahini, S. A. (2017). EEG activities and the sustained attention performance. *Neurophysiology*, 49(3), 226–233. <https://doi.org/10.1007/s11062-017-9675-1>
- Bui, T., & Das, J. M. (2022). *Neuroanatomy, Cerebral hemisphere*. StatPearls Publishing.
- Cheng, B., Fan, C., Fu, H., Huang, J., Chen, H., & Luo, X. (2022). Measuring and computing cognitive statuses of construction workers based on electroencephalogram: A critical review. *IEEE Transactions on Computational Social Systems*, 9(6), 1644–1659. <https://doi.org/10.1109/TCSS.2022.3158585>
- Garrett, J. W., & Teizer, J. (2009). Human factors analysis classification system relating to human error awareness taxonomy in construction safety. *Journal of Construction Engineering and Management*, 135(8), 754–763. [https://doi.org/doi:10.1061/\(ASCE\)CO.1943-7862.0000034](https://doi.org/doi:10.1061/(ASCE)CO.1943-7862.0000034)
- Gong, P., Guo, H., Yuanyue, H., & Guo, S. (2020). Safety risk evaluations of deep foundation construction schemes based on imbalanced data sets. *Journal of Civil Engineering and Management*, 26(4), 380–395. <https://doi.org/10.3846/jcem.2020.12321>
- Hall, M., Frank, E., Holmes, G., Pfahringer, B., Reutemann, P., & Witten, I. H. (2009). The WEKA data mining software: An update. *ACM SIGKDD Explorations Newsletter*, 11(1), 10–18. <https://doi.org/10.1145/1656274.1656278>
- Hosmer Jr, D. W., Lemeshow, S., & Sturdivant, R. X. (2013). *Applied logistic regression* (3rd ed.). John Wiley & Sons. <https://doi.org/10.1002/9781118548387>
- Huang, C. X., Shi, N. L., Miao, Y. N., Chen, X. G., Wang, Y. J., & Gao, X. R. (2024). Visual tracking brain-computer interface. *Iscience*, 27(4), Article 109376. <https://doi.org/10.1016/j.isci.2024.109376>
- Ince, R., Adanir, S. S., & Sevmez, F. (2021). The inventor of electroencephalography (EEG): Hans Berger (1873–1941). *Child's Nervous System*, 37, 2723–2724. <https://doi.org/10.1007/s00381-020-04564-z>
- Klem, G. H., Lüders, H. O., Jasper, H. H., & Elger, C. (1961). The ten twenty electrode system: International Federation of Societies for Electroencephalography and Clinical Neurophysiology. *American Journal of EEG Technology*, 1(1), 13–19. <https://doi.org/10.1080/00029238.1961.11080571>
- Occupational Safety and Health Administration. (2020). *109 Labor inspection statistics annual report*. Ministry of Labor, Taiwan.
- Larsen, O. F. P., Tresselt, W. G., Lorenz, E. A., Holt, T., Sandstrak, G., Hansen, T. I., Su, X. M., & Holt, A. (2024). A method for synchronized use of EEG and eye tracking in fully immersive VR. *Frontiers in Human Neuroscience*, 18. <https://doi.org/10.3389/fnhum.2024.1347974>
- Liao, P.-C., Zhou, X., Chong, H.-Y., Yinan, H., & Zhang, D. (2022). Exploring construction workers' brain connectivity during hazard recognition: A cognitive psychology perspective. *International Journal of Occupational Safety and Ergonomics*, 29(1), 207–215. <https://doi.org/10.1080/10803548.2022.2035966>
- Liu, X., Hu, B. L., Si, Y., & Wang, Q. (2024). The role of eye movement signals in non-invasive brain-computer interface typing system. *Medical & Biological Engineering & Computing*, 62, 1981–1990. <https://doi.org/10.1007/s11517-024-03070-7>
- Liu, Y., Chen, H., & Wang, X. (2021). Risk prediction and diagnosis of water seepage in operational shield tunnels based on random forest. *Journal of Civil Engineering and Management*, 27(5), 539–552. <https://doi.org/10.3846/jcem.2021.14901>
- McCulloch, W. S., & Pitts, W. (1943). A logical calculus of the ideas immanent in nervous activity. *The Bulletin of Mathematical Biophysics*, 5(4), 115–133. <https://doi.org/10.1007/BF02478259>
- Mohamed, W. N. H. W., Salleh, M. N. M., & Omar, A. H. (2012). A comparative study of Reduced Error Pruning method in decision tree algorithms. In *2012 IEEE International Conference on Control System, Computing and Engineering*, Penang, Malaysia. <https://doi.org/10.1109/ICCSC.2012.6487177>
- Moore II, D. H. (1987). Classification and regression trees, by Leo Breiman, Jerome H. Friedman, Richard A. Olshen, and Charles J. Stone. Brooks/Cole Publishing, Monterey, 1984, 358 pages, \$27.95. *Cytometry*, 8(5), 534–535. <https://doi.org/10.1002/cyto.990080516>
- Noghbaei, M., Han, K., & Albert, A. (2021). Feasibility study to identify brain activity and eye-tracking features for assessing hazard recognition using consumer-grade wearables in an immersive virtual environment. *Construction Engineering and Management*, 147(9), Article 04021104. [https://doi.org/10.1061/\(ASCE\)CO.1943-7862.0002130](https://doi.org/10.1061/(ASCE)CO.1943-7862.0002130)
- Rosen, K. H., & Krithivasan, K. (2012). *Discrete mathematics and its applications: with combinatorics and graph theory*. Tata McGraw-Hill Education.
- Saedi, S., Fini, A. A. F., Khanzadi, M., Wong, J., Sheikhhoshkar, M., & Banaei, M. (2022). Applications of electroencephalography in construction. *Automation in Construction*, 133, Article 103985. <https://doi.org/10.1016/j.autcon.2021.103985>
- Saghafi, A., Tsokos, C. P., Goudarzi, M., & Farhizadeh, H. (2017). Random eye state change detection in real-time using EEG signals. *Expert Systems with Applications*, 72, 42–48. <https://doi.org/10.1016/j.eswa.2016.12.010>
- Smola, A., & Vapnik, V. (1997). Support vector regression machines. In *NIPS'96: Proceedings of the 9th International Conference on Neural Information Processing Systems* (pp. 155–161), Denver, CO, USA. <https://dl.acm.org/doi/10.5555/2998981.2999003>
- Vecchiato, G., Toppi, J., Astolfi, L., De Vico Fallani, F., Cincotti, F., Mattia, D., Bez, F., & Babiloni, F. (2011). Spectral EEG frontal asymmetries correlate with the experienced pleasantness of TV commercial advertisements. *Medical & Biological Engineering & Computing*, 49(5), 579–583. <https://doi.org/10.1007/s11517-011-0747-x>
- Vortmann, L.-M., Ceh, S., & Putze, F. (2022). Multimodal EEG and eye tracking feature fusion approaches for attention classification in hybrid BCIs. *Frontiers in Computer Science*, 4. <https://doi.org/10.3389/fcomp.2022.780580>
- Wei, C.-C. (2021). Collapse warning system using LSTM neural networks for construction disaster prevention in extreme wind weather. *Journal of Civil Engineering and Management*, 27(4), 230–245. <https://doi.org/10.3846/jcem.2021.14649>

## APPENDIX

Table A1. WEKA parameter settings

Machine learning model	Parameter	Parameter value
Decision tree (J48)	BatchSize	100
	MinNum	2
	NumDecimalPlaces	2
	NumFolds	3
	Seed	1
Bayesian network (BayesNet)	Batch size	100
	Estimator	SimpleEstimator
	Number of decimal places	2
	Search algorithm	K2
Artificial neural networks (Multilayer Perceptron, MLP)	Batch size	100
	Learning rate	0.3
	Momentum	0.2
	Training time	500
	Validation threshold	20
REPTree	BatchSize	100
	InitialCount	0.0
	MaxDepth	-1
	MinNum	2.0
	MinVarianceProp	0.001
	NumDecimalPlaces	2
	NumFolds	3
	Seed	1
Logistic regression	Batch size	100
	Number of decimal places	4
	Ridge	1.0E-8
Support vector machine (SMO)	BatchSize	100
	C	1.0
	Kernel	PolyKernel
	NumDecimalPlaces	2
	NumFolds	-1
RandomForest	BatchSize	100
	MaxDepth	0
	NumDecimalPlaces	2
	NumFeatures	0
	Seed	1

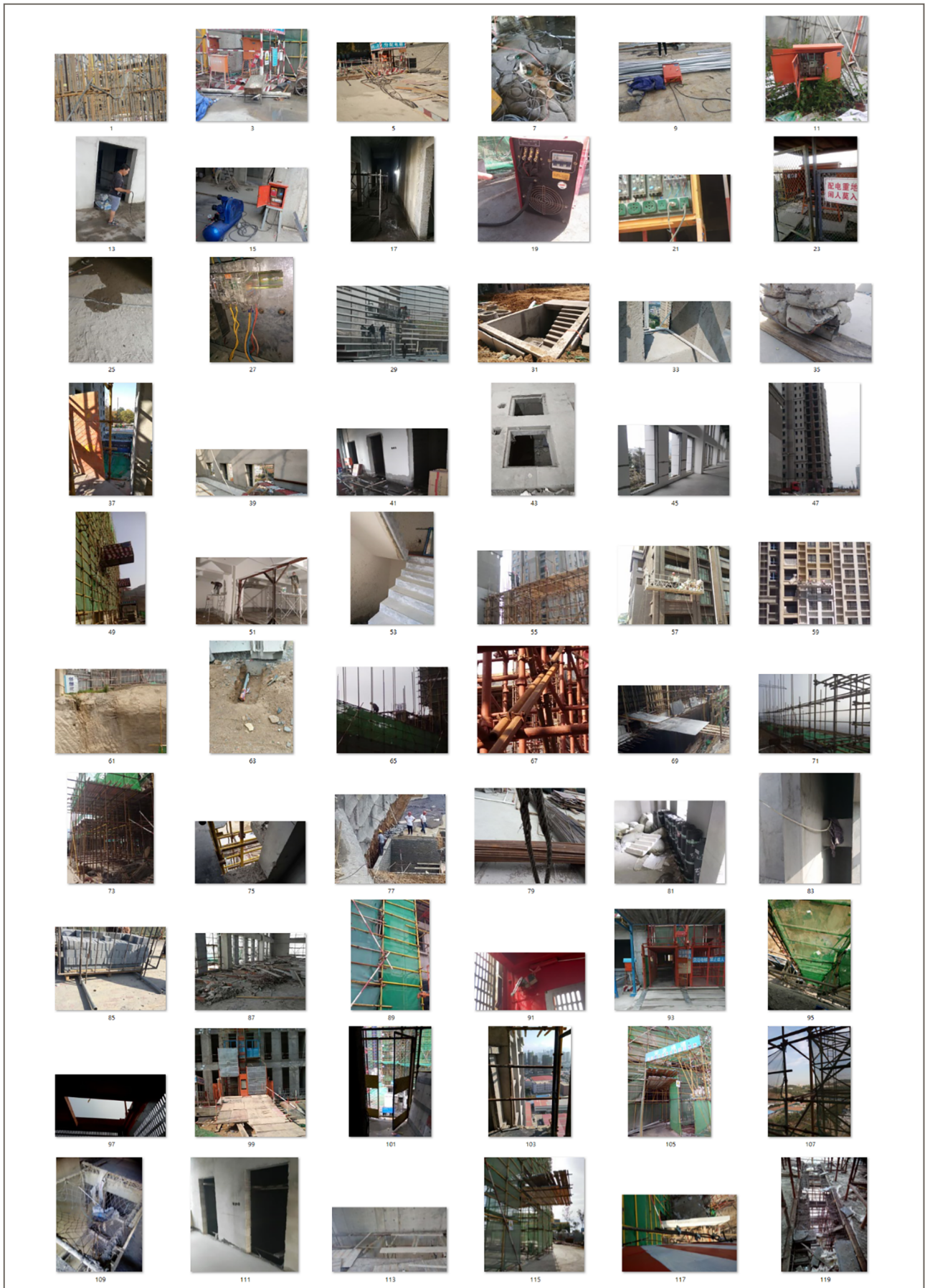


Figure A1. Examples of hazardous conditions at construction sites

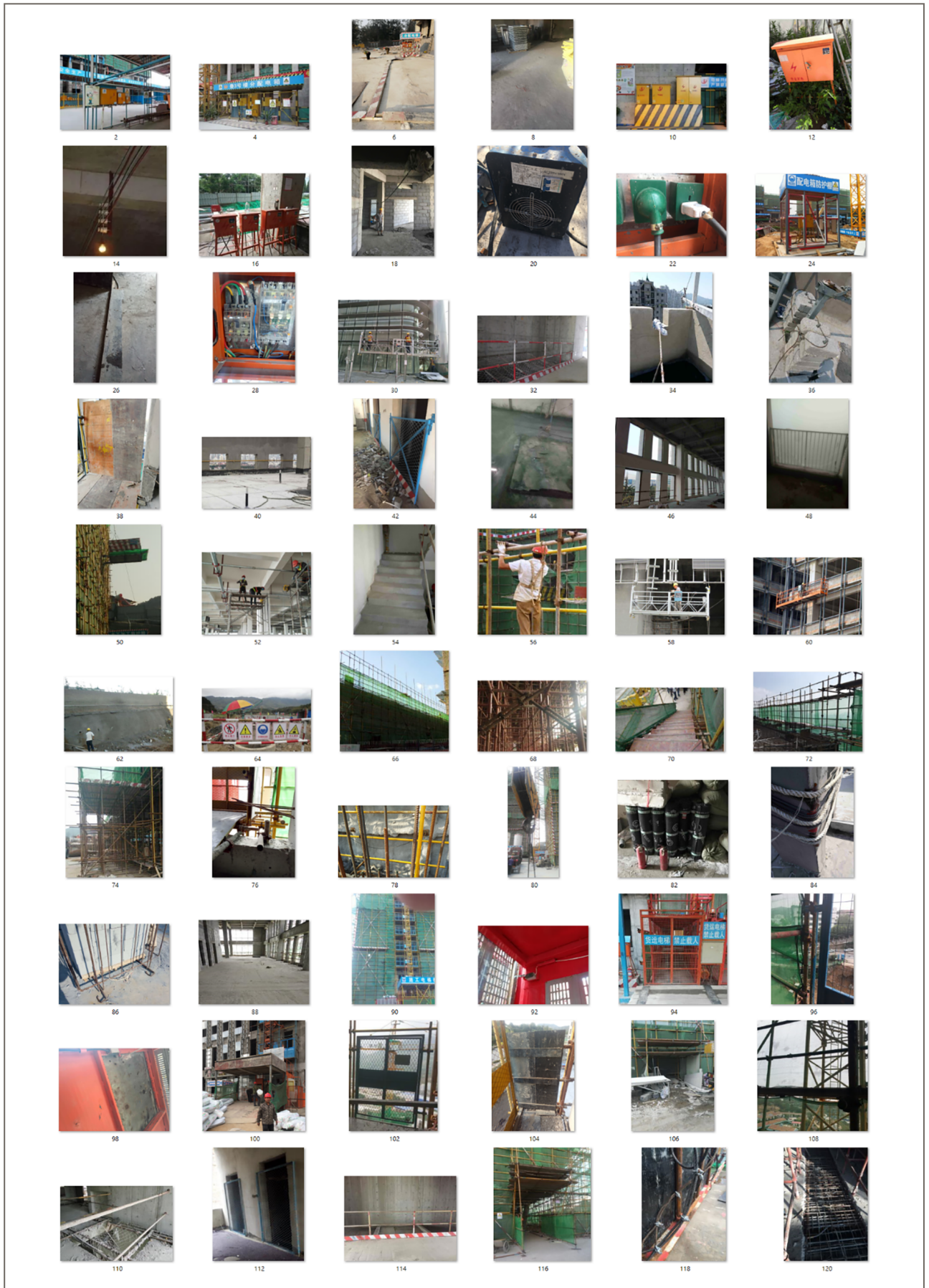


Figure A2. Examples of safety practices at construction sites